Reproduction and Breeding 3 (2023) 199–207

Contents lists available at ScienceDirect

Reproduction and Breeding

journal homepage: www.keaipublishing.com/en/journals/reproduction-and-breeding

A regression approach for assessing large molecular drug concentration in breast milk

Allesandra Stratigakis [a,1], Dylan Paty [a,1], Peng Zou [b], Zhongyuan Zhao [a], Yanyan Li [c], Tao Zhang [a,*]

[a] Department of Pharmaceutical Sciences, SUNY-Binghamton University, 96 Corliss Ave, Johnson City, NY, 13790, USA
[b] Daiichi Sankyo, Inc., 211 Mount Airy Road, Basking Ridge, NJ, 07920, USA
[c] School of Food and Agriculture, College of Natural Sciences, Forestry, and Agriculture, University of Maine, Orono, ME, 04469, USA

ARTICLE INFO

Keywords:
Regression model
Milk to plasma concentration ratio (M/P)
Large molecule drugs
Breast milk
Lactation
Pharmacokinetics

ABSTRACT

The development of an effective method for predicting the transfer of biologics from plasma into breast milk is important to ensure the safe use of medications during lactation. The aim of this study was to develop a regression model that could predict the transfer of monoclonal antibodies (mAbs) and Fc-fusion proteins from plasma into breast milk. By searching various databases, a list of eleven mAbs and Fc-fusion proteins with available information of presence in the breast milk was generated. Physicochemical properties such as the isoelectric point (pI), molecular weight (MW), dissociation constant (K_d), and pharmacokinetic (PK) parameters such as clearance (CL), volume of distribution (V_d), and half-life ($T_{1/2}$) were collected or calculated. A two-variable non-linear regression analysis and a multivariate regression analysis were employed to establish correlation of milk-to-plasma (M/P) ratios with different combinations of two physicochemical properties. The 3D isoelectric point (pI) of the Fv region and the buried surface area (BSA) between the light and heavy chains (LC_HC) were two factors that emerged as a promising predictor of the milk-to-plasma concentration ratio (M/P). The correlation between M/P ratio, 3D pI of Fv region, and BSA_LC_HC was found to be good with R^2 of 0.9058. Other combinations of the physicochemical properties did not show a statistically significant correlation. The multivariate regression model was used to predict the MP ratios for 79 different mAbs. We believe that this regression model could serve as a valuable tool to estimate the M/P ratios of mAbs and Fc-fusion proteins. Further model validation is necessary when the M/P ratios of additional biologics are available. This could inform clinical decision-making and improve the safety of large molecule drug use during lactation.

1. Introduction

Making the best evidence-based clinical decision regarding maternal drug use during breastfeeding remains an ongoing challenge. Many drugs may be considered safe to use during lactation, however, high-quality human data regarding short-term and long-term risks and benefits of the drugs on the exposed infants are still limited. Information on how much a drug can be deposited into breast milk are critical to improve clinical decision-making. Despite extensive efforts to enhance drug labeling for safe use during lactation, only 5.2 % of drug labels approved between 2003 and 2012 contained information related to human lactation [1]. Previously, several quantitative structure-activity relationship (QSAR) methods have been used to predict drug milk-to-plasma (M/P) ratios [2–7]. Recently, a few new in vitro to in vivo extrapolation (IVIVE) and PBPK modeling methods have emerged to predict the transfer of drugs into breast milk [8–14]. In addition, mouse and human mammary epithelial cell-based permeability assays have also been devised to estimate the milk-to-plasma (M/P)

Abbreviations: AUC, Area under the curve; Avg_HI, Average Hydrophobic Imbalance; BSA_LC_HC, Surface area buried between VL and VH domains; CL, Clearance; DM.HM, Ratio of dipole moment to hydrophobic moment; FcRn, Neonatal Fc receptor; Fv, variable domain; K_d, dissociation constant; M/P, Milk to plasma; mAbs, Monoclonal antibodies; MW, Molecular weight; pI, Isoelectric point; PK, Pharmacokinetic; $T_{1/2}$, Half-life; V_d, Volume of distribution.

* Corresponding author. School of Pharmacy and Pharmaceutical Sciences, SUNY-Binghamton University, 96 Corliss Ave, Johnson City, NY, 13790, USA.
E-mail addresses: astrati1@binghamton.edu (A. Stratigakis), dpaty1@binghamton.edu (D. Paty), pzou@dsi.com (P. Zou), zzhao62@binghamton.edu (Z. Zhao), yanyan.li@maine.edu (Y. Li), zhangt@binghamton.edu (T. Zhang).

[1] Both authors contribute equally to this work.

https://doi.org/10.1016/j.repbre.2023.10.003
Received 15 August 2023; Received in revised form 13 October 2023; Accepted 20 October 2023
Available online 10 November 2023

concentration ratios of some drugs [12,15]. However, despite these advances, challenges such as cost, time, and limitations such as inter-species variability and limited pharmacokinetic data in human milk can still pose a hindrance in obtaining enough evidence-based information to guide the decision of whether to discontinue breastfeeding while taking medications [16]. Therefore, without knowledge of the drug concentration in human milk, regulatory bodies and healthcare professionals find it challenging to make decisions about drug therapy and the continuation of breastfeeding during treatment. Furthermore, these approaches were all developed for small-molecule drugs.

Therapeutic protein drugs have recently been at the forefront of drug development as they offer treatment options for medical conditions thought to have limited options [17]. Depending on drug classes and indications, many of these therapeutic proteins are commonly used as immunosuppressive therapies in autoimmune diseases or as oncological therapies. In several studies, it has been discovered that low levels of therapeutic protein drugs may be present in breast milk produced by women who take these medications [18]. Previous research suggested that the use of therapeutic proteins in nursing women is unlikely to pose a serious safety risk to infants probably because of the low amount of therapeutic proteins in milk and limited oral absorption of therapeutic proteins in the infant's gastrointestinal tract [19]. However, the potential safety risk of therapeutic proteins in milk to breastfed infants cannot be excluded because of limited clinical safety and pharmacokinetic (PK) data.

While therapeutic proteins are not expected to be excreted into milk by passive diffusion, neonatal Fc receptor (FcRn)-mediated transcytosis may contribute to the transport of monoclonal antibodies (mAbs) and Fc-fusion or albumin-fusion proteins into breast milk. This receptor protects Immunoglobulin G (IgG) from degradation by binding the IgG Fc domain, allowing them to be transported back to the cell's surface and released into circulation. This process operates in acidic environments and is known as the FcRn-transcytosis pathway [20]. Additionally, overt mastitis and perhaps other inflammatory conditions in the mother can disrupt membranes, which allows substances such as drugs, large molecules, and lipids, to enter milk in amounts greater than anticipated [21]. FcRn is expressed by human intestinal epithelial cells in both the fetus and adult as well [22]. Human FcRn-mediated IgG transcytosis may facilitate oral absorption of therapeutic mAbs and Fc-fusion or albumin-fusion proteins, especially in newborns due to reduced proteolysis of IgG by trypsin, increased FcRn-mediated IgG transcytosis in neonatal enterocytes, and immature mucosal barriers until after weaning [22]. Therefore, although the concentrations of therapeutic mAbs and Fc-fusion or albumin-fusion proteins in human milk are usually low, the use of therapeutic proteins in nursing women may pose a potential safety risk on breastfed newborns.

The physicochemical properties of different therapeutic proteins can significantly impact their PK and toxicity profiles. These physicochemical characteristics of drugs may impact their transfer into breast milk as well [23]. Such properties include isoelectric point (pI), molecular weight (MW), FcRn dissociation constant (K_d), and so on. The isoelectric point (pI) is reported to directly impact an antibody's pharmacokinetic and pharmacodynamic activity when administered to the body [24]. When pI is more positively charged, subcutaneous absorption of the mAbs is greatly reduced due to less repulsion endured encountering the more negatively charged extracellular matrix [25]. FcRn binding affinity is well-documented to prolong the half-lives of Fc-containing proteins, contributing to their decreased degradation within the body [26]. Therefore, it is possible that those parameters may potentially infer the transfer of large molecule drugs into breast milk. Therefore, the objectives of this research are to explore the correlations between M/P ratio of therapeutic proteins and their physicochemical properties using publicly available data and use the established correlation model to predict the human M/P ratios of approved therapeutic proteins and therapeutic proteins under clinical development.

2. Methods

2.1. Collection of M/P ratios and in vitro parameter data

To select the drugs of interest, a preliminary list of approved and under-reviewed monoclonal antibodies (mAbs) was first obtained from the Antibody Society's website [27]. Then more drugs were included through search results from published papers from Pubmed database and Drugs and Lactation Database [28,29]. The final list of 11 mAbs with human milk concentration data available is shown in Table 1, and they are adalimumab, belimumab, bevacizumab, certolizumab, infliximab, ipilimumab, natalizumab, rituximab, tocilizumab, ustekinumab, and vedolizumab.

Physicochemical properties such as the isoelectric point (pI), molecular weight (MW), dissociation constant (K_d), and pharmacokinetic (PK) parameters such as clearance (CL), volume of distribution (V_d), and half-life ($T_{1/2}$) were collected or calculated for selected mAbs as summarized in Table 1. Isoelectric pI and MW of the drugs were estimated based on heavy and light polypeptide chain sequences. For adalimumab, infliximab, ipilimumab, natalizumab, rituximab, ustekinumab, bevacizumab, and belimumab, this information was gathered from the NCBI website using their non-proprietary names [30]. DrugBank [31] was used to get the amino acid sequences for certolizumab, vedolizumab and tocilizumab. The ExPASy calculator was then used to estimate the pI and MW using amino acid sequences of heavy and light chains of these drugs [32]. The pI's of the rest of the large-molecule drugs were collected directly from DrugBank. FcRn K_d values for Rituximab, Bevacizumab, Tocilizumab, Vedolzimab, Adalimumab, Natalizumab and Infliximab were obtained from Taylor and Francis Online [20]. The clearance (CL), volume of distribution (V_d) and elimination half-life ($T_{1/2}$) for all drugs were collected from DrugBank [31]. The isoelectric point of the antigen-binding region for each of the investigated monoclonal antibodies (Fab pI), the structure-based pI of Fv (variable domain) region (3D pI of Fv region), the ratio of surface areas of charged patches to hydrophobic patches (patch ratio), the ratio of dipole moment to hydrophobic moment (DM.HM), and average hydrophobic imbalance (Avg HI) values were obtained from The Antibody Society [24].

The estimation of M/P ratios for those drugs were conducted using different approaches depending on available information. The concentrations of Adalimumab, Bevacizumab, Natalizumab, and Ustekinumab in maternal serum and breast milk were obtained from Ben-Horin et al.'s study [33], Ehlken et al.'s study [34], Baker et al.'s study [35], Bar-Gil Shitrit et al.'s study [36], respectively. For those drugs, the concentration time profiles of adalimumab in serum and milk were digitized using WebDigitizer (GNU Affero General Public License Version 3) and the

Table 1
Calculated M/P ratios of 11 mAbs based on data found from literature.

mAb	Calculated M/P	Ref.	Mean M/P
Adalimumab	0.0042	[57]	0.0042
Belimumab	0.0041 (2 wk post 1st dose) 0.0022 (1 day after 2nd dose) 0.0035 (1 wk post 2nd dose)	[58]	0.0033
Bevacizumab	0.0090	[59]	0.0090
Certolizumab	0.0016	[60,61]	0.0016
Infliximab	0.0033	[57]	0.0033
Ipilimumab	0.0015	[62]	0.0015
Natalizumab	0.00096 (Mother 2) 0.0028 (Mother 3)	[63]	0.0019
Rituximab	0.0040	[64]	0.0040
Tocilizumab	0.00082 (max) 0.00045 [65]	[58]	0.00064
Ustekinumab	0.0021 (Patient 1) 0.0048 (Patient 2) .00034 (Patient 3)	[66]	0.0024
Vedolizumab	0.022 (max) 0.0040	[41] [65]	0.013

area under the curve (AUC) was estimated using PKAnalysis (Lixoft, Batiment D, Antony, France). The M/P ratios were estimated based on AUC ratios of milk over plasma. For the rest of drugs, Belimumab [37] Infliximab [38], Ipilimumab [38], Rituximab [39], Tocilizumab [40], Vedolizumab [41–43], usually only one drug concentration in the milk at a single time point or only the maximum and/or minimum concentrations were reported. For those drugs, the M/P ratios were estimated based on milk to plasma drug concentration ratio at one time point. In the case of more than one time point was reported, the average M/P ratios were used as the final M/P ratio.

2.2. Regression analysis and M/P prediction

To investigate the relationship between the physicochemical properties and M/P ratios, a two-variable regression analysis was used to evaluate the correlation of each physicochemical property with M/P ratios of the drugs first. Then a multivariate regression analysis was employed to establish correlation of M/P ratios with different combinations of two physicochemical properties.

For the multivariate regression analysis, we are using R studio to do the regression analysis and using AIC to be the variable selection criteria, we tested several approaches such as mutilinear regression, Paraboloid regression, Gaussian regression and Lorentzian regression [44,45]. Then we use AIC, R square, and Residual Standard Error as criteria to select the best model. Eventually we used 3D pI of Fv region and BSA_LC_HC to estimate the M/P ratio using Lorentzian regression as shown below.

$$M \Big/ P\ ratio = \frac{a}{\left(\left(1+\left(\frac{(x-x_0)}{b}\right)^2\right)\right)\left(\left(1+\left(\frac{(y-y_0)}{c}\right)^2\right)\right)}$$

After fitting the data in we can identify $a, b, c, x_0, and y_0$, which a is the height of Lorentzian curve, b and c are the shape and width of the Lorentzian curve which are all get from the Lorentzian regression model. x_0 and y_0 are the mean of PI_3D and BSA_LC_HC.

The final nonlinear multivariate regression model was selected and used to predict the human M/P ratios of 72 approved full-length monoclonal antibodies on the market. The data for the Surface Area Buried between V_L and V_H Domains (BSA_LC_HC) and 3D pI of Fv region were obtained from Ahmed, L., et al.'s study [24]. The drug list and parameters were shown in Table 5.

3. Results

The collected information and the estimated parameters regarding the physicochemical properties of 11 large-molecule drugs were summarized in Table 2. Molecular weight of the drugs ranged from 91 to 149 kD. The M/P ratio ranged from 0.0015 to 0.013. The Equilibrium Dissociation Constant (K_d) reflects the drugs' FcRn binding affinity [25]. The K_d values ranged from 0.28 to 1.18 M, although for some drugs this information is not available. The isoelectric point (pI) is the pH of a system for an antibody to have no net electrical charge [46]. This parameter is an indicator of overall charge of an IgG, which affects the absorption and distribution of IgG's in the body due to electrical repulsions/attractions when interacting with charged regions during circulation and clearance. The calculated pI values for the current list of drugs ranged from 6.9 to 9.2, which suggests that some may be positively charged while others are negatively charged at physiological pH. The Fab pI value is the isoelectric point (overall electrical charge) of the Fab fragment for each of the investigated monoclonal antibodies/immunoglobulins. This electrical charge plays a role in being the most differentiated/unique/variable portion of an IgGs identity and ability to bind to antigens/toxins, which provoke an immune response within the body, typically resulting in the decreased bioavailability of the IgG in question [47]. The Fab pI values ranged from 5.8 to 9.2. The Structure-based pI of Fv region (3D pI) is a computationally calculated approximation of the overall isoelectric point of the variable region of each of the IgGs, providing an alternative structure-based calculation of their charges when in biological pH. This value has also been correlated with the aggregation potential and viscosity of IgGs, causing alterations in solution viscosity both in vitro and PK/PD in vivo [48]. The 3D pI of the Fv region ranged from 5.48 to 9.33. Both Fab pI and 3D pI values span a wider range compared to pI values, which may suggest these two

Table 3
Statistics of the linear regression analysis of physicochemical properties for M/P ratio correlation.

Property	R∩2	Adjusted R∩2	SE
pI	0.00004	−0.11107	0.00374
Fab pI	0.20722	0.11913	0.00333
3D pI of Fv region	0.12484	0.02760	0.00350
Molecular weight (g/mol)	0.06999	−0.03335	0.00361
BSA_LC_HC	0.52225	0.46917	0.00259
Kd	0.00014	−0.19983	0.00440
PatchRatio (RP)	0.00055	−0.11050	0.00374
DM.HM (RM)	0.00177	−0.10914	0.00374
Avg_HI	0.00635	−0.10405	0.00373

Table 4
Statistics of the multivariable regression analysis of physicochemical properties for M/P ratio correlation.

Property 1	Property 2	R	Rsqr	Adj Rsqr	SE
3D pI of Fv region	BSA_LC_HC	0.9517	0.9058	0.8430	0.0014
DM. HM	BSA_LC_HC	0.7540	0.5685	0.4606	0.0026
Fab pI	BSA_LC_HC	0.8227	0.6768	0.5960	0.0023
Fab pI	DM. HM	0.6223	0.3873	0.2341	0.0031
BSA_LC_HC	DM. HM	0.7540	0.5685	0.4606	0.0026

Table 2
Parameters of physicochemical properties of 11 large-molecule drugs.

Drug Name	M/P	pI	Fab pI	3D pI of Fv region	Molecular weight (g/mol)	BSA_LC_HC	Kd	PatchRatio (RP)	DM. HM (RM)	Avg_HI	Volume of Distribution (L)	Clearance (mL/d/kg)	Half-life (days)
Adalimumab	0.0042	8.4	8.5	8.05	144,190	733.17	1.18	2.274	0.584	1.17	5.35	4.1	14
Belimumab	0.0033	8.3	7.2	7.43	147,000	775.26	NA	2.266	1.68	0.891	5.29	4.1	14
Bevacizumab	0.0090	8.3	7.2	6.79	149,000	811.49	0.50	1.395	1.27	1.42	2.84	3.1	20
Certolizumab	0.0016	6.9	8.0	7.59	91,000	750.27	NA	1.153	0.378	1.92	6.00	4.8	14
Infliximab	0.0033	7.3	5.8	5.48	144,190	755.50	0.80	1.794	2.58	0.686	3.50	4.5	8.6
Ipilimumab	0.0015	9.2	8.9	8.97	148,000	763.75	NA	1.387	1.60	0.852	7.21	5.2	14
Natalizumab	0.0026	7.9	8.7	8.68	144,190	835.94	0.28	1.904	0.257	1.23	5.45	5.5	11
Rituximab	0.0040	8.7	9.1	9.33	143,859	848.38	0.46	1.868	0.487	0.801	3.80	4.8	18
Tocilizumab	0.0021	8.6	9.2	9.14	148,000	750.80	0.46	1.314	1.16	1.24	6.93	4.3	22
Ustekinumab	0.0024	8.5	8.9	8.50	148,600	797.38	NA	1.611	0.495	1.16	4.51	4.0	22
Vedolizumab	0.013	8.1	7.0	7.39	146,837	916.05	0.60	1.570	0.751	1.21	4.49	2.2	15

Table 5
Predicted M/P ratio of 79 large molecule drugs with BSA_LC_HC and pI_3D values.

Antibody	BSA_LC_HC	pI_3D	Predicted M/P
abciximab	844.41754	4.284668	0.00343906
adalimumab	733.16583	8.0454102	0.00192667
alemtuzumab	859.50189	9.4956055	0.00306408
alirocumab	769.60223	7.7084961	0.00351772
atezolizumab	798.46857	7.2250977	0.00635821
avelumab	861.26422	8.2797852	0.00653409
basiliximab	715.14966	9.3637695	0.00070867
belimumab	775.25665	7.4301758	0.00440073
benralizumab	785.61047	8.5727539	0.00240805
bevacizumab	811.48926	6.7856445	0.00834178
Bezlotoxumab	767.55719	8.9536133	0.00154322
blinatumomab_FV1	963.70929	4.9829102	0.00372197
blinatumomab_FV2	728.92273	8.675293	0.00122393
brentuximab	838.40845	4.6401367	0.00403091
brodalumab	827.85187	9.2026367	0.00267744
burosumab	734.13794	8.1479492	0.00181830
canakinumab	787.62823	7.7817383	0.00413188
cemiplimab	764.72382	7.4008789	0.00397046
certolizumab	750.26672	7.5913086	0.00305745
cetuximab	719.18469	7.7670898	0.00201243
daclizumab	744.73724	8.675293	0.00143578
daratumumab	804.86322	7.4594727	0.00612237
denosumab	784.70941	8.7338867	0.00215018
dinutuximab	629.50006	8.7045898	0.00052646
dupilumab	943.37036	7.8110352	0.00679001
durvalumab	699.6474	7.6352539	0.00182402
eculizumab	777.43848	5.2241211	0.00292374
efalizumab	884.15082	8.5727539	0.00591235
elotuzumab	818.02759	6.4174805	0.00878878
emicizumab_FV1	817.35138	5.300293	0.00490834
emicizumab_FV2	955.45917	9.0708008	0.00264217
erenumab	870.41437	9.4516602	0.00334876
evolocumab	666.15643	7.4887695	0.00149997
fremanezumab	796.59839	7.5620117	0.00524357
galcanezumab	694.9801	8.7924805	0.00083036
gemtuzumab	712.28088	7.5620117	0.00213477
golimumab	872.75848	8.9243164	0.00460395
guselkumab	763.8385	8.7192383	0.00171299
Ibalizumab	749.71741	6.8149414	0.0041120
ibritumomab	854.23798	9.1879883	0.0035054
idarucizumab	833.55054	8.6020508	0.00412112
infliximab	755.50378	5.4780273	0.00270588
inotuzumab	1046.4897	8.7631836	0.00115661
ipilimumab	763.74902	8.9682617	0.00146632
itolizumab	772.23804	8.5141602	0.00214549
ixekizumab	820.73151	8.8364258	0.00307891
lanadelumab	801.92267	8.4262695	0.00320845
mepolizumab	835.58875	8.1186523	0.00578082
mogamulizumab	777.88409	7.6352539	0.00403906
moxetumomab	1026.4858	5.7954102	0.00306333
muromonab	732.81982	8.9389648	0.00107905
natalizumab	835.93890	8.6752930	0.00403394
necitumumab	723.79895	7.8256836	0.00202684
nimotuzumab	727.04578	8.5727539	0.00128321
nivolumab	617.94574	8.9096680	0.00042785
obiltoxaximab	867.74976	8.8950195	0.00457901
obinutuzumab	764.05157	7.6352539	0.00345731
ocrelizumab	876.02948	8.4262695	0.00639257
ofatumumab	791.48633	8.0454102	0.00364581
olaratumab	860.08356	8.1040039	0.00727916
omalizumab	877.55310	5.4780273	0.00919751
palivizumab	799.24695	8.8510742	0.00237001
panitumumab	644.43860	5.1479492	0.00080874
pembrolizumab	720.80682	8.3676758	0.00138088
pertuzumab	806.19122	8.4116211	0.00340723
racotumomab	914.75403	5.8842773	0.01080501
ramucirumab	648.27631	8.5141602	0.0006811
ranibizumab	778.86249	6.1889648	0.00517502
reslizumab	814.97571	6.7856445	0.00869040
rituximab	848.37549	9.3344727	0.00306334
sarilumab	762.81201	7.5180664	0.00365012
secukinumab	827.86859	7.5766602	0.00748945
siltuximab	829.18848	7.7817383	0.00671089
tildrakizumab	706.40106	8.2944336	0.00126735
tocilizumab	750.79553	9.1440430	0.00114751
tositumomab	857.50201	9.2758789	0.00341722
trastuzumab	735.69757	8.4116211	0.00155237
ustekinumab	797.38416	8.4995117	0.00289899
vedolizumab	916.04840	7.3862305	0.01120678

parameters may be more sensitive properties of the large molecule drugs than pI. This is supported by the high R2 in the two variable regression analysis (Fig. 1A–C).

The Surface Area Buried between V_L and V_H Domains (BSA_LC_HC) represents the buried surface area between the variable light and heavy domains of the Fv region. This value indicates how the interaction between these two domains contributes to the Fv region's stability and correlates to compatibility between them. A smaller buried surface area between the V_L and V_H domains has been shown to decrease the conformational stability of the Fv region at any given temperature [49]. The BSA_LC_HC values ranged from 733 to 916. The dissociation constant, K_d, is a measure of the affinity between a ligand and its binding partner, determining the strength of the interaction. K_d represents the concentration of ligand required to occupy half of the available binding sites. A lower K_d value indicates a stronger binding affinity [50]. The available K_d values ranged from 0.28 to 1.18 M [51]. Adalimumab is anti-tumor necrosis factor (TNF) biological agent with a higher K_d than the rest of drugs [52]. It is likely due to a larger buried surface and an epitope that extensively occupies the binding area in comparison to other biologics Other TNF biologics (infliximab and certolizumab) included in this study do not show this.

The Ratio of Surface Areas of Charged Patches to Hydrophobic patches (PatchRatio) is the overall ratio of positively and negatively charged patches compared to hydrophobic molecular surface patches. It has been shown to influence the behavior of an antibody when in solution [53]. More specifically, the large hydrophobic and charged patches have been correlated with increased viscosity and excess aggregation when using different antibodies [25]. The PatchRatio values ranged from 1.314 to 2.274. The Ratio of Dipole Moment to Hydrophobic Moment (DM.HM) is the ratio of concentration-dependent reactions. These values are generated by solute-solute as well as solute-solvent interactions, which involve polar and nonpolar domains. A dipole moment represents the separation of positive and negatively charged residues in a biologic system, while hydrophobic moment represents the separation of hydrophobic and hydrophilic residues in a biologic system [24]. These types of interactions greatly affect the bioavailability of the IgG due to alternative interaction besides distribution/circulation. The DM.HM values ranged from 0.257 to 2.576. The Average Hydrophobic Imbalance (Avg_HI) measures how directionally dependent the distribution of hydrophobic residues are on the surface of a protein. A lower Avg_HI value indicates even distribution of the hydrophobic residues, while a higher value indicates localization of the hydrophobic residues in a region on the surface on the protein. The Avg_HI values ranged from 0.686 to 1.916.

With regard to PK parameters, the clearance for mAbs is usually slow, and in the current list of drugs the values ranged from 2.2 to 54.5 mL/day/kg BW. The Volume of Distribution (V_d) values are small as well (ranged from 2.84 to 7.21 L) due to the large size of those drugs. Half-life (T1/2) of a drug is determined by CL and Vd, which shows how long a drug stays in the systemic circulation. The T1/2 of the 13 drugs ranged from 4.25 to 21.5 days.

The outcomes of the regression analyses between M/P and physiochemical properties can be seen in Fig. 1 and were summarized in Table 3. From the model we got a is 0.0152, b is 1.5134, and c is 84.4682. And x_0 is 6.6786, y_0 is 887.6552. No statistically significant correlation was observed through these bivariate regressions, indicates

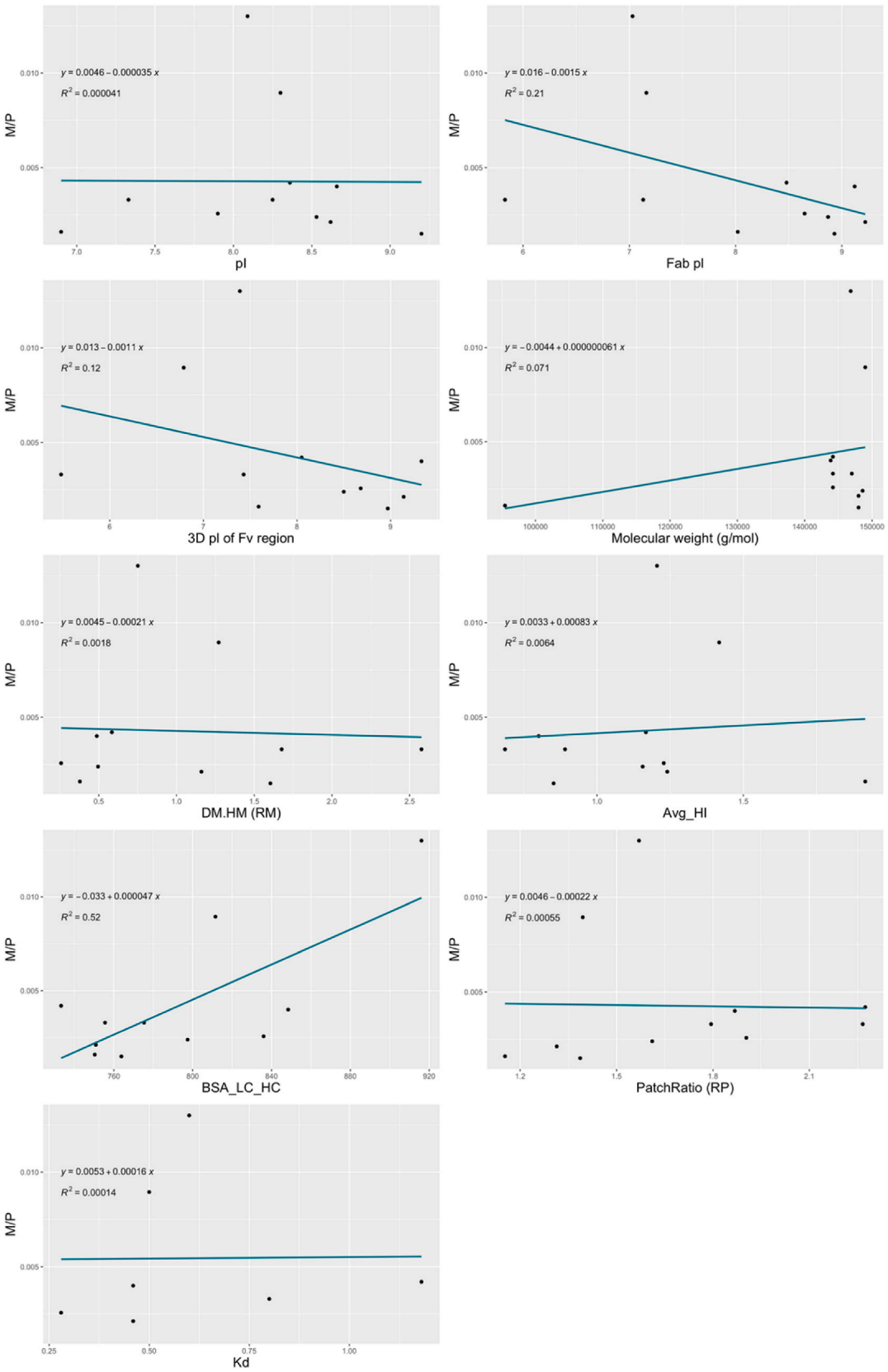

Fig. 1. Linear relationships between M/P ration and physiochemical properties: isoelectric point (pI) (A), investigated monoclonal antibodies (Fab pI) (B), 3D pI of Fv region (C), molecular weight (D), The data for the Surface Area Buried between V_L and V_H Domains (BSA_LC_HC) (E), PatchRatio (F), the ratio of dipole moment to hydrophobic moment (DM.HM) (G), average hydrophobic imbalance (Avg_HI) (H), and FcRn dissociation constant (Kd) (I). Correlation equations are shown in the plot. R^2 means the percentage of information contained in this regression model.

that M/P ratio is not solely dependent on a single physiochemical property in Table 3. Based on the two factors regression analyses result, multivariate regression was conducted for selected factors.

Results of the multivariate regression analysis of M/P were summarized in Table 4. The correlation between M/P ratio, 3D pI of Fv region, and BSA_LC_HC was found to be good with R^2 of 0.9058. The 3-D regression plot is shown in Fig. 2. Other combinations of the physicochemical properties did not show a statistically significant correlation.

The multivariate regression model was used to predict the MP ratios for 79 different mAbs and the results were shown in Table 5. The 3D plot of correlation between predicted M/P ratio, 3D pI of Fv region, and BSA_LC_HC were plotted in Fig. 3. The predicted M/P ratios for those large molecule drugs range from 0.0003 to 0.0151, indicating a relatively low presence in human breast milk in general compared with small molecule drugs. The predicted M/P ratios and the observed M/P ratios are reported in Table 6.

4. Discussion

The present study investigated various physiochemical properties of approved marketed biotherapeutic drugs to establish a correlation of them with the milk-to-plasma ratios. Our multivariate analysis showed that 3D pI of Fv region, and BSA_LC_HC have a statistically significant correlation with M/P ratios of 11 large molecule mAbs.

Previous research has suggested the possible mechanism of transport of large-molecule drugs into breast milk. During the first 3–4 days after delivery when colostrum is produced, spaces are created between mammary epithelial cells, allowing relatively larger molecules like mAbs and cells like leukocytes to freely pass from the maternal circulation to the breast milk at this time. Lactogenesis II takes place following the colostral phase, which leads to increased milk production and the gradual closure of intracellular spaces. Without these open pores, drugs can only enter the milk by passively diffusing down a concentration gradient created by the nonionized, unbound drug on either side of the membrane that functions as a semipermeable lipid barrier [54]. Larger drug molecules must dissolve in the outer lipid membrane of epithelial cells, diffuse across the aqueous interior, and pass through the membrane of the neighboring cell, before passing into the milk. Therefore, molecules that are too large or highly charged can no longer passively diffuse into breastmilk [23].

Another important consideration in determining the relative bioavailability of a drug in the transfer to breast milk is the neonatal crystallizable fragment receptor (FcRn) binding affinity. This receptor protects Immunoglobulin G (IgG) from degradation by binding the IgG Fc domain, allowing them to be transported back to the cell's surface and released into circulation. This process operates in acidic environments and is known as the FcRn-transcytosis pathway [20]. In addition, FcRn binding affinity is well-documented to prolong the half-lives of Fc-containing proteins, contributing to their decreased degradation within the body.

The physicochemical properties of different therapeutic proteins can significantly impact their pharmacokinetic (PK) and toxicity profiles. These physicochemical characteristics of drugs could be valuable in determining their milk-to-plasma ratio [23]. Isoelectric point (pI) is reported to directly impact an antibody's pharmacokinetic and pharmacodynamic activity [24]. When pI is more positively charged, subcutaneous absorption of the drug molecule can be greatly reduced due to less repulsion endured encountering the more negatively charged extracellular matrix [25].

Furthermore, previous studies have shown that structure-based pI calculations, such as 3D pI, proves the most accurate charge calculation for antibodies [48]. This highlights the dependability of the 3D pI calculations when considering the electrostatic properties of antibody molecules, confirming our focus on this physicochemical feature, rather than other pI calculations, as essential for characterizing antibody charge properties.

Because most mAbs have the same amino acid sequence for the same isotype in the constant region of the Fc domain, the variable-domain (Fv) region, which is made up of both the variable heavy (VH) and variable light (VL) domains and can be visualized in Fig. 4, was focused on as a way of specific differentiation of the charge and interaction properties for the selected IgGs [55]. The pI of the Fv region has been shown to impact the aggregation potential and viscosity of IgGs when in solution, with more negatively charged regions correlating with an increased solution viscosity and aggregation potential [48].

Additionally, the stability of the F_V domain, is impacted by the interactions between the two domains. The stability reflects the degree to which the two are compatible with each other, meaning a smaller

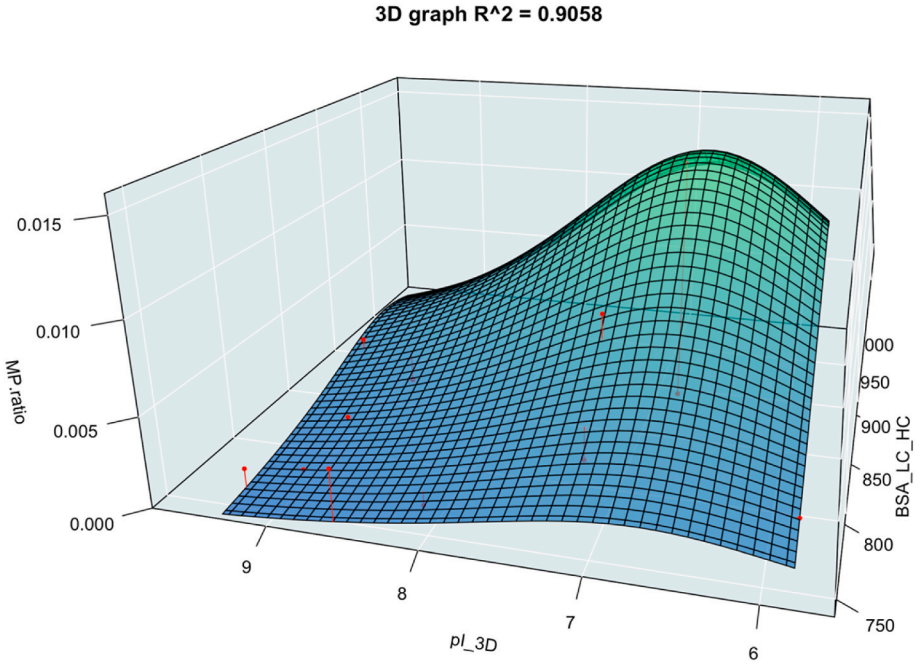

Fig. 2. The 3D plot of correlation between observed M/P ratio, 3D pI of Fv region, and BSA_LC_HC of 11 large molecule drugs.

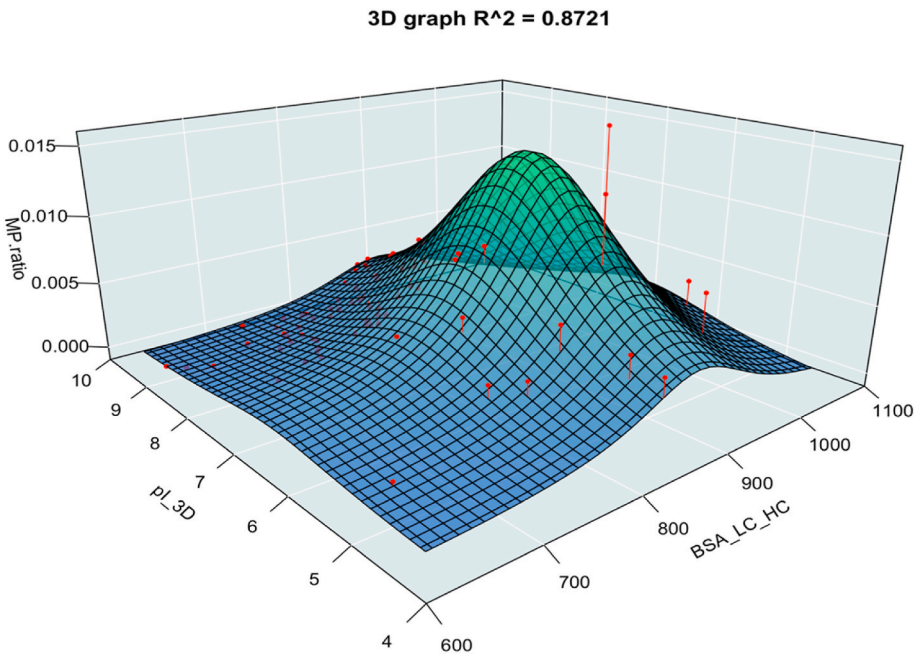

Fig. 3. The 3D plot of correlation between predicted M/P ratio, 3D pI of Fv region, and BSA_LC_HC of 79 large molecule drugs.

Table 6
Predicted M/P ratio of 12 large molecule drugs.

Antibody	Observed M/P	Predicted M/P	Residual
Adalimumab	0.0042	0.001447	2.75E-03
Belimumab	0.0033	0.005038	−1.74E-03
Bevacizumab	0.00895	0.007613	1.34E-03
Certolizumab	0.0016	0.002335	−7.35E-04
Infliximab	0.0033	0.003354	−5.40E-05
Ipilimumab	0.0015	0.001501	−9.60E-07
Natalizumab	0.00257	0.0041	−1.53E-03
Omalizumab	0.00104	0.014874	−1.38E-02
Rituximab	0.004	0.003469	5.31E-04
Tocilizumab	0.00212	0.001098	1.02E-03
Ustekinumab	0.00239	0.002291	9.87E-05
blinatumomab_FV1	963.70929	4.9829102	0.00372197

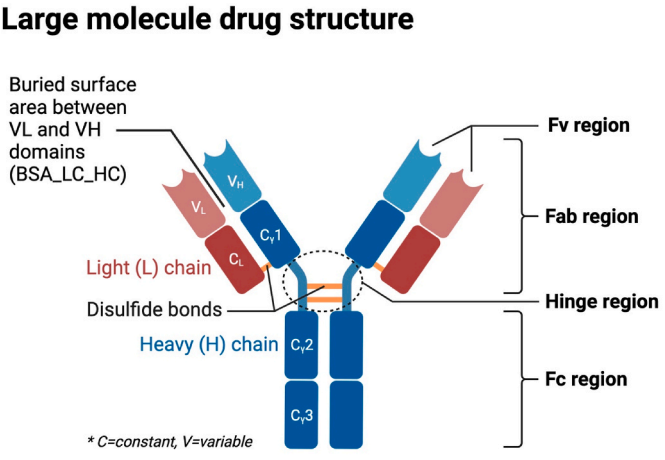

Fig. 4. A visual representation of a large molecule drug/mAb.

surface area between the two regions (VH and VL) correlates with reduced conformational stability of the FV region and leads to a reduced antigen-binding affinity. This surface area is defined as BSA_LC_HC, based on the interactions of the variable domains [24]. The BSA_LC_HC serves as a measure of the stability of the Fv region. This stability can affect the degradation of mAbs in the mammary gland, meaning that mAbs with a lower BSA_LC_HC and thus a less stable Fv region may be more likely to be degraded in the mammary gland, which could lead to decreased transport of the large molecule drugs into breast milk [56]. Using the observed surface area between the two domains, the relative prediction of binding affinity, and the stability of the F_V region can prove to be reliable physicochemical properties for comparing various mAbs and estimating pharmacokinetic effects, such as M/P ratio.

Pharmacokinetic (PK) parameters, such as clearance, half-life, and volume of distribution, describe the dynamic behavior of drugs in the body. While PK parameters provide important information about how drugs are absorbed, distributed, metabolized, and eliminated from the body, they are an indirect way to predict the milk to plasma concentration ratio (M/P ratio) of drugs since the PK profile of a drug is determined by its physiochemical properties. Therefore, the correlation of PK parameters with M/P ratios were not shown here.

Our study revealed that a single parameter doesn't correlate with M/P ratios, but multivariate analysis is more predictive of M/P ratios. The good correlation of 3D pI of Fv region and BSA_LC_HC with M/P ratios highlights the complex relationship between the physicochemical properties of Fv region (i.e., binding affinity, stability, and charge) and mammary excretion of IgG, and emphasizes the need for further analysis. This research may shed light on the development of more accurate and dependable methods for predicting the transfer of large molecule drugs from serum to breast milk. With the growing use of biologics, it is crucial to have a better understanding of the potential effects on infants during pregnancy and postpartum.

5. Conclusion

A regression model was developed to predict the M/P ratio of mAbs using 3D pI of the Fv region and BSA_ LC_HC. This regression model can be a useful tool for predicting M/P ratios of mAbs. Further validation of the model can be done when more mAbs have M/P information available.

Funding support

This research did not receive any specific grant from funding agencies in the public, commercial, or not-for-profit sectors.

Previous presentations of the work

This manuscript represents original work and has not been presented previously. The work has not been accepted for publication, published previously, nor is under consideration for publication by another journal.

CRediT authorship contribution statement

Allesandra Stratigakis: Data curation, Writing – original draft, Writing – review & editing. **Dylan Paty:** Data curation, Writing – original draft. **Peng Zou:** Conceptualization, Methodology, Supervision, Writing – review & editing. **Zhongyuan Zhao:** Data curation, Writing – review & editing. **Yanyan Li:** Conceptualization, Writing – review & editing. **Tao Zhang:** Conceptualization, Data curation, Methodology, Supervision, Writing – review & editing.

Declaration of competing interest

All authors declare no conflicts of interest relevant to the content of this article.

References

[1] J. Wang, et al., Evaluation of the safety of drugs and biological products used during lactation: workshop summary, Clin. Pharmacol. Ther. 101 (6) (2017) 736–744.
[2] E.J. Begg, H.C. Atkinson, Modelling of the passage of drugs into milk, Pharmacol. Ther. 59 (3) (1993) 301–310.
[3] H.C. Atkinson, E.J. Begg, Prediction of drug concentrations in human skim milk from plasma protein binding and acid-base characteristics, Br. J. Clin. Pharmacol. 25 (4) (1988) 495–503.
[4] H.C. Atkinson, E.J. Begg, Prediction of drug distribution into human milk from physicochemical characteristics, Clin. Pharmacokinet. 18 (2) (1990) 151–167.
[5] J.C. Fleishaker, N. Desai, P.J. McNamara, Factors affecting the milk-to-plasma drug concentration ratio in lactating women: physical interactions with protein and fat, J. Pharmaceut. Sci. 76 (3) (1987) 189–193.
[6] L.A. Larsen, S. Ito, G. Koren, Prediction of milk/plasma concentration ratio of drugs, Ann. Pharmacother. 37 (9) (2003) 1299–1306.
[7] H. Koshimichi, et al., Analysis and prediction of drug transfer into human milk taking into consideration secretion and reuptake clearances across the mammary epithelia, Drug Metab. Dispos. 39 (12) (2011) 2370–2380.
[8] S.R. Delaney, et al., Predicting escitalopram exposure to breastfeeding infants: integrating analytical and in silico techniques, Clin. Pharmacokinet. 57 (12) (2018) 1603–1611.
[9] A. Olagunju, et al., Physiologically-based pharmacokinetic modelling of infant exposure to efavirenz through breastfeeding, AAS Open Research 1 (16) (2018) 1–19.
[10] K. Abduljalil, et al., Prediction of drug concentrations in milk during breastfeeding, integrating predictive algorithms within a physiologically-based pharmacokinetic model, CPT Pharmacometrics Syst. Pharmacol. 10 (8) (2021) 878–889.
[11] T. Zhang, et al., Physiologically based pharmacokinetic model to predict drug concentrations of breast cancer resistance protein substrates in milk, Biopharm. Drug 43 (6) (2022) 221–232.
[12] T. Zhang, et al., An in vitro human mammary epithelial cell permeability assay to assess drug secretion into breast milk, Int. J. Pharm. X 4 (2022), 100122.
[13] H. Yang, et al., Developing an in vitro to in vivo extrapolation (IVIVE) model to predict human milk-to-plasma drug concentration ratios, Mol. Pharm. 19 (7) (2022) 2506–2517.
[14] K. Abduljalil, I. Gardner, M. Jamei, Application of a physiologically based pharmacokinetic Approach to predict theophylline pharmacokinetics using virtual non-pregnant, pregnant, fetal, breast-feeding, and neonatal populations, Front Pediatr 10 (2022), 840710.
[15] M.A. Athavale, et al., Development of an in vitro cell culture model to study milk to plasma ratios of therapeutic drugs, Indian J. Pharmacol. 45 (4) (2013) 325–329.
[16] F.J. Nice, A.C. Luo, Medications and breast-feeding: current concepts, J Am Pharm Assoc (2003) 52 (1) (2012) 86–94.
[17] L. Urquhart, Top companies and drugs by sales in 2021, Nat. Rev. Drug Discov. 21 (4) (2022) 251.
[18] E. Klenske, et al., Drug levels in the maternal serum, cord blood and breast milk of a ustekinumab-treated patient with crohn's disease, J Crohns Colitis 13 (2) (2019) 267–269.
[19] C. Gotestam Skorpen, et al., The EULAR points to consider for use of antirheumatic drugs before pregnancy, and during pregnancy and lactation, Ann. Rheum. Dis. 75 (5) (2016) 795–810.
[20] S. Chung, et al., An in vitro FcRn- dependent transcytosis assay as a screening tool for predictive assessment of nonspecific clearance of antibody therapeutics in humans, mAbs 11 (5) (2019) 942–955.
[21] K.M. Hunt, et al., Mastitis is associated with increased free fatty acids, somatic cell count, and interleukin-8 concentrations in human milk, Breastfeed. Med. 8 (1) (2013) 105–110.
[22] D.C. Roopenian, S. Akilesh, FcRn: the neonatal Fc receptor comes of age, Nat. Rev. Immunol. 7 (9) (2007) 715–725.
[23] P.O. Anderson, Drugs in lactation, Pharm Res 35 (3) (2018) 45.
[24] L. Ahmed, et al., Intrinsic physicochemical profile of marketed antibody-based biotherapeutics, Proc. Natl. Acad. Sci. U.S.A. 118 (37) (2021).
[25] A. Datta-Mannan, et al., Influence of physiochemical properties on the subcutaneous absorption and bioavailability of monoclonal antibodies, mAbs 12 (1) (2020), 1770028.
[26] M. Pyzik, et al., FcRn: the architect behind the immune and nonimmune functions of IgG and albumin, J. Immunol. 194 (10) (2015) 4595–4603.
[27] Society, T.A. Antibody Society. Available from: https://www.antibodysociety.org/..
[28] LactMed, Drugs And Lactation Database (LactMed®), 2006. Available from: https://www.ncbi.nlm.nih.gov/books/NBK501922/.
[29] Pubmed. *PubMed*. Available from: https://pubmed.ncbi.nlm.nih.gov/.
[30] Information, T.N.C.f.B, The national center for biotechnology information, Available from: https://www.ncbi.nlm.nih.gov/.
[31] D. Online, DrugBank Online, 2006. Available from: https://go.drugbank.com/.
[32] C.G. Séverine Duvaud, Frédérique Lisacek, Heinz Stockinger, Vassilios Ioannidis, Christine Durinx, Expasy, the Swiss Bioinformatics Resource Portal, 2021 *as designed by its users*.
[33] S. Ben–Horin, et al., Adalimumab level in breast milk of a nursing mother, Clin. Gastroenterol. Hepatol. 8 (5) (2010) 475–476.
[34] C. Ehlken, et al., Reduction of vascular endothelial growth factor A in human breast milk after intravitreal injection of bevacizumab but not ranibizumab, Arch. Ophthalmol. 130 (9) (2012) 1226–1227.
[35] T.E. Baker, et al., Transfer of natalizumab into breast milk in a mother with multiple sclerosis, J. Hum. Lactation 31 (2) (2015) 233–236.
[36] A. Bar-Gil Shitrit, et al., Detection of ustekinumab in breast milk of nursing mothers with crohn disease, Inflamm. Bowel Dis. 27 (5) (2021) 742–745.
[37] J. Saito, et al., Belimumab concentrations in maternal serum and breast milk during breastfeeding and the safety assessment of the infant: a case study, Breastfeed. Med. 15 (7) (2020) 475–477.
[38] E. Ross, et al., Therapeutic monoclonal antibodies in human breast milk: a case study, Melanoma Res. 24 (2) (2014) 177–180.
[39] Y. Bragnes, et al., Low level of Rituximab in human breast milk in a patient treated during lactation, Rheumatology 56 (6) (2017) 1047–1048.
[40] J. Saito, et al., Tocilizumab concentrations in maternal serum and breast milk during breastfeeding and a safety assessment in infants: a case study, Rheumatology 57 (8) (2018) 1499–1501.
[41] W. Sun, et al., Vedolizumab concentrations in breast milk: results from a prospective, postmarketing, milk-only lactation study in nursing mothers with inflammatory bowel disease, Clin. Pharmacokinet. 60 (6) (2021) 811–818.
[42] B.G. Feagan, et al., Vedolizumab as induction and maintenance therapy for ulcerative colitis, N. Engl. J. Med. 369 (8) (2013) 699–710.
[43] W.J. Sandborn, et al., Vedolizumab as induction and maintenance therapy for Crohn's disease, N. Engl. J. Med. 369 (8) (2013) 711–721.
[44] S. Yoshioka, Y. Aso, S. Kojima, Softening temperature of lyophilized bovine serum albumin and gamma-globulin as measured by spin-spin relaxation time of protein protons, J. Pharmaceut. Sci. 86 (4) (1997) 470–474.
[45] W.A. Pansera, et al., Nonlinear regression using Gaussian-Lorentzian functions to empirical modeling of convective-diffusive chloride transport in concrete, Construct. Build. Mater. 341 (2022), 127770.
[46] Z. Schenider, Importance of Isoelectric point(pI) of Antibodies, The Antibody Society, 2017 [cited 2022.
[47] H.W. Schroeder Jr., L. Cavacini, Structure and function of immunoglobulins, J. Allergy Clin. Immunol. 125 (2 Suppl 2) (2010) S41–S52.
[48] N. Thorsteinson, et al., Structure-based charge calculations for predicting isoelectric point, viscosity, clearance, and profiling antibody therapeutics, mAbs 13 (1) (2021), 1981805.
[49] S. Müller-Späth, et al., From the Cover: charge interactions can dominate the dimensions of intrinsically disordered proteins, Proc. Natl. Acad. Sci. U.S.A. 107 (33) (2010) 14609–14614.
[50] T. Gerecsei, et al., Dissociation constant of integrin-RGD binding in live cells from automated micropipette and label-free optical data, Biosensors (Basel) 11 (2) (2021).
[51] S. Hu, et al., Comparison of the inhibition mechanisms of adalimumab and infliximab in treating tumor necrosis factor α-associated diseases from a molecular view*, J. Biol. Chem. 288 (38) (2013) 27059–27067.
[52] S.P. Reddy, et al., Chapter 8 - etanercept, in: J.J. Wu, S.R. Feldman, M.G. Lebwohl (Eds.), Therapy for Severe Psoriasis, Elsevier, 2016, pp. 83–96.
[53] P. Nichols, et al., Rational design of viscosity reducing mutants of a monoclonal antibody: hydrophobic versus electrostatic inter-molecular interactions, mAbs 7 (1) (2015) 212–230.
[54] P.O. Anderson, J.B. Sauberan, Modeling drug passage into human milk, Clin. Pharmacol. Ther. 100 (1) (2016) 42–52.

[55] A.B. Kuhn, et al., Improved solution-state properties of monoclonal antibodies by targeted mutations, J. Phys. Chem. B 121 (48) (2017) 10818–10827.
[56] J.A. Marsh, Buried and accessible surface area control intrinsic protein flexibility, J. Mol. Biol. 425 (17) (2013) 3250–3263.
[57] S. Ben-Horin, et al., The immunogenic part of infliximab is the F(ab')2, but measuring antibodies to the intact infliximab molecule is more clinically useful, Gut 60 (1) (2011) 41–48.
[58] J. Saito, et al., Tocilizumab during pregnancy and lactation: drug levels in maternal serum, cord blood, breast milk and infant serum, Rheumatology (Oxford) 58 (8) (2019) 1505–1507.
[59] C. Ehlken, et al., Reduction of vascular endothelial growth factor a in human breast milk after intravitreal injection of bevacizumab but not ranibizumab, Arch. Ophthalmol. 130 (9) (2012) 1226–1227.
[60] M.E. Clowse, et al., Minimal to no transfer of certolizumab pegol into breast milk: results from CRADLE, a prospective, postmarketing, multicentre, pharmacokinetic study, Ann. Rheum. Dis. 76 (11) (2017) 1890–1896.
[61] FDA, CIMZIA (Certolizumab Pegol) for Injection, for Subcutaneous Use, 2008.
[62] E. Ross, et al., Therapeutic monoclonal antibodies in human breast milk: a case study, Melanoma Res. 24 (2) (2014) 177–180.
[63] T.E. Baker, et al., Transfer of natalizumab into breast milk in a mother with multiple sclerosis, J. Hum. Lactation 31 (2) (2015) 233–236.
[64] Y. Bragnes, et al., Low level of Rituximab in human breast milk in a patient treated during lactation, Rheumatology (Oxford) 56 (6) (2017) 1047–1048.
[65] K. Zhang, et al., The establishment of a highly sensitive ELISA for detecting bovine serum albumin (BSA) based on a specific pair of monoclonal antibodies (mAb) and its application in vaccine quality control, Hum. Vaccine 6 (8) (2010) 652–658.
[66] A. Bar-Gil Shitrit, et al., Detection of ustekinumab in breast milk of nursing mothers with crohn disease, Inflamm. Bowel Dis. 27 (5) (2021) 742–745.